

Cite this article as: Hao Juan, Yang Chao, Jiang Bailing, et al. Effects of Magnetron Sputtering Techniques on Microstructure and Mechanical Properties of Nanocrystalline TiN Films[J]. Rare Metal Materials and Engineering, 2021, 50(08): 2715-2720.

ARTICLE

Effects of Magnetron Sputtering Techniques on Microstructure and Mechanical Properties of Nanocrystalline TiN Films

Hao Juan¹, Yang Chao¹, Jiang Bailing¹, Du Yuzhou¹, Wang Rong¹, Wang Xu¹, Zhou Kesong²

¹ School of Material Science and Engineering, Xi'an University of Technology, Xi'an 710048, China; ² Institute of New Materials, Guangdong Academy of Sciences, Guangzhou 510651, China

Abstract: The structure and properties of nanocrystalline TiN films deposited by direct current magnetron sputtering (dcMS), high power pulsed magnetron sputtering (HPPMS) and modulated pulsed power magnetron sputtering (MPPMS) were compared. Results show that columnar structure with a few gaps is obtained through dcMS because of low ionization rate and low kinetic energy of sputtered species, which results in poor mechanical properties; the deposition rate is 51 nm/min. The TiN film deposited by HPPMS exhibits dense structure and smooth surface, which is because HPPMS can improve ionization rate of sputtered species under the conditions of high peak target power and low duty cycle. The mechanical properties are improved, but the average deposition rate is relatively low, only 25 nm/min. MPPMS has the capability to modulate peak target power and duty cycle to achieve high ionization degree and deposition rate. Thus, the TiN film deposited by MPPMS shows dense columnar structure, smooth surface, superior mechanical properties and enhanced deposition rate of 45 nm/min.

Key words: MPPMS; TiN films; microstructure; deposition rate

TiN films have good mechanical properties, low electrical resistivity, excellent chemical and thermal stability, and have been applied in the fields such as abrasion-resistant film on tool steels, diffusion barrier layers in semiconductor devices, and flat panel displays^[1-4]. Dc magnetron sputtering (dcMS) has been widely used in the field of TiN film preparation for many years. The target materials can be widely selected and the target current can be precisely controlled in dcMS process^[5-7], which is commonly applied to prepare multi-layer gradient or metallic compound thin films at low deposition temperature. However, the ionization rate and kinetic energy of sputtered species in dcMS plasma are generally low. A porous film with a poor adhesion is always obtained under the low ion flux and ion energy conditions^[8].

Structure and mechanical properties of TiN films are sensitive to ion flux and ion energy of sputtered species, which are closely related to the deposition process and target

power^[9]. High power pulsed magnetron sputtering (HPPMS) is a technique to obtain highly ionized plasma by applying high peak power density (such as 1~3 kW/cm²) to the target in a short time (such as microseconds)^[10-12]. Compared with dcMS, HPPMS can deposit films with compact structure, good adhesion and improved mechanical properties^[13]. However, the average deposition rate of HPPMS is extremely low^[14].

Several years ago, Chistyakov proposed a new technique of modulated pulsed power magnetron sputtering (MPPMS)^[15-17]. MPPMS not only obtains highly ionized plasma, but also overcomes the loss of deposition rate by adopting the high peak target power density and long pulse width. In addition, MPPMS utilizes multiple steps and micro pulse in one pulse period to decrease average target power and to avoid overheating of target. Meanwhile, MPPMS can arbitrarily modify pulse shape to achieve various plasma characteristics and stable discharge for different target materials.

Received date: August 10, 2020

Foundation item: National Natural Science Foundation of China (51271144, 51571114)

Corresponding author: Yang Chao, Ph. D., Lecturer, School of Material Science and Engineering, Xi'an University of Technology, Xi'an 710048, P. R. China, Tel: 0086-29-82312812, E-mail: yangchao0107@sina.com

Copyright © 2021, Northwest Institute for Nonferrous Metal Research. Published by Science Press. All rights reserved.

Most researchers have done a lot of work on the influence of deposition parameters on the microstructure and properties of TiN films. Correlation between different deposition techniques, plasma characteristics and the resultant structure and properties of TiN films is rarely investigated. Therefore, we selected dcMS, HPPMS and MPPMS techniques to prepare nano TiN films under the same target power, and compared the structure and mechanical properties. Specifically, in order to avoid that the deposition parameters selected for comparison might benefit one technique, many references had been used for the setting of deposition parameters^[18-20].

1 Experiment

TiN films were deposited in a closed field unbalanced magnetron sputtering (CFUBMS) system using a circle Ti target ($\Phi 130$ mm, thickness 8 mm, purity 99.9%). Cathodic magnetrons of dcMS, HPPMS and MPPMS were driven by continuous dc power, homemade high power pulsed power and modulated pulsed power, respectively, in power regulation mode. Silicon and AISI 304 stainless steel were used as substrates. Before the experiment, the substrates were ultrasonically cleaned in alcohol for 15 min and then installed into substrate holder. The distance from target to substrate was 130 mm. The vacuum chamber was pumped down to a base pressure of 1.0×10^{-4} Pa.

In the deposition, substrate surface was cleaned by Ar⁺ etching at a working pressure of 0.5 Pa with a pulsed dc substrate bias voltage of -450 V (250 kHz and 87.5% duty cycle) for 15 min. A Ti transition layer with thickness of 200~300 nm was deposited for improving adhesion between TiN layer and substrate. TiN films with similar thickness were reactively deposited using dcMS, HPPMS and MPPMS techniques from metal Ti target in an Ar/N₂ mixture with Ar:N₂ flow ratio of 3:1. The working pressure was 0.8 Pa. Average target power of 2.5 kW and substrate bias voltage of -65 V (40 kHz and 98% duty cycle) were used in the depositions. The detailed preparation parameters are listed in Table 1.

The crystal structure of TiN films was characterized by XRD (XRD-7000S, Shimadzu Limited Corp.) using Cu K α radiation (45 kV and 40 mA) in the range of 30°~80° with 0.02° increment. The chemical compositions were investigated by X-ray photoelectron spectroscopy (AXIS ULTRA, Kratos Analytical Ltd.). The surface and cross-sectional structure morphologies were observed by field-emission SEM (JSM-6700F, JEOL Ltd). The microstructure was examined by high-resolution transmission electron

microscope (JEM-3010, JEOL Ltd). The surface roughness was measured using an atomic force microscope (SPI3800-SPA-400, Seiko Instruments Inc) for an area of 25 μm^2 . The hardness and Young's modulus of TiN films were measured using nanoindenter (G200, Agilent Technologies) equipped with a Berkovich diamond indenter. The indentation depth was kept constantly below 10% of the film thickness to minimize the substrate effect^[21]. The residual stress was measured by an IC flatness and wafer stress analyzer (BGS-6341, Beijing Institute of Opto-Electronic Technology). The adhesion was evaluated by microscratch tester (WS-2005, ZKKH Instruments Inc.) at applied load from 0 N to 60 N. When the coating cracks for the first time, the corresponding load is the critical load. The scratch track and film failure morphology were characterized by optical microscope (GX71, OLYMPUS Inc).

2 Results and Discussion

2.1 Deposition rate

Fig. 1 shows the average deposition rate of TiN films deposited by dcMS, HPPMS and MPPMS, which is 51, 25 and 45 nm/min, respectively. The deposition rate of dcMS is the highest and that of HPPMS is the lowest.

Two aspects should be considered to explain the change of the average deposition rate. In the deposition process of HPPMS and MPPMS, a part of deposited ions can be attracted back toward the target and captured by high negative potential of the cathode which is used to induce high density plasma. Therefore, deposition rate of HPPMS and MPPMS is lower than that of dcMS. In addition, power source of HPPMS is designed to deliver voltage pulse with a rectangular shape, i.e. a constant voltage during the pulse on-time. However, discharge current shows a slow increase, which leads to a decrease in actual deposition time^[22]. In comparison, MPPMS technique can utilize multiple stages (weakly ionized stage and strongly ionized stage) in one MPP pulse to accelerate the increasing speed of discharge current and to reduce the discharge voltage. Thus, the deposition rate of TiN films deposited by MPPMS is improved.

2.2 Microstructure

Fig.2 shows XRD patterns of TiN films deposited by dcMS, HPPMS and MPPMS. All TiN films exhibit NaCl-type face center cubic (fcc) structure with (111), (200), (220) and (311) crystal face based on JCPDS card 38-1420#. However, the intensity and broadening of diffraction peaks for three group TiN films show remarkable difference. Grain sizes of TiN films are estimated using the Scherrer formula^[23]. Grain sizes

Table 1 Preparation parameters of TiN films deposited by dcMS, HPPMS and MPPMS

| Technique | Pulsing parameters | p_a/kW | p_p/kW | $p/\text{kW}\cdot\text{cm}^2$ | I/A | U/V | i/A | $T/^\circ\text{C}$ | t/min |
|-----------|--------------------------|-----------------|-----------------|-------------------------------|--------------|--------------|--------------|--------------------|----------------|
| dcMS | - | 2.5 | 2.5 | 0.01 | 7.1 | 354 | 0.3 | 173 | 90 |
| HPPMS | 50 Hz and 10% duty cycle | 2.5 | 25.3 | 0.60 | 40.5 | 625 | 0.1 | 146 | 180 |
| MPPMS | 50 Hz and 18% duty cycle | 2.5 | 27.5 | 0.65 | 45 | 610 | 0.1 | 170 | 120 |

Note: p_a -average target power; p_p -peak target power; p -peak target power density; I -peak target current; U -peak target voltage; i -substrate current; T -deposition temperature; t -deposition time

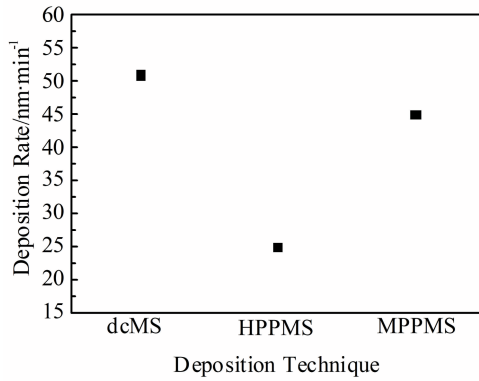


Fig.1 Average deposition rates of TiN films deposited by dcMS, HPPMS and MPPMS

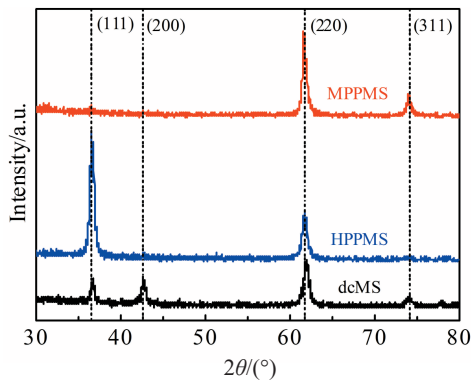


Fig.2 XRD patterns of TiN films deposited by dcMS, HPPMS and MPPMS

of TiN films deposited by dcMS, HPPMS and MPPMS are estimated to be 14, 15 and 19 nm, respectively. Diffraction peaks of the TiN film deposited by dcMS shift to higher angle compared to standard diffraction peaks, which should be related to its tensile residual stress of 0.3 GPa (Table 2).

Plasma characteristics markedly affect preferred orientation of TiN films. As shown in Fig.2, TiN films deposited by dcMS and MPPMS exhibit (220) preferred orientation, while HPPMS shows (111) preferred orientation. Formation of preferred orientation during film growth is a complex process which can be explained by thermodynamics and kinetics. Thermodynamics effect is based on the principle of minimization of the overall energy in terms of a competition among surface energy, strain energy and stopping energy. (200) plane has the lowest surface energy, (111) plane has the lowest strain

energy and (220) plane has the lowest stopping energy^[24]. In general, grains are oriented with their faster growing directions perpendicular to the surface, which will overgrow the slower growing grains by competitive grain growth. In this growth model, grains will grow on low surface energy (200) plane to minimize the surface energy. However, when additional kinetic or thermal energy is incorporated into deposition process, adatom will receive higher momentum transfer and gain higher mobility to move around, resulting in the production of (111) orientation which is the lowest strain energy plane. As ionization rate of HPPMS increases, improved ion bombardment will increase adatom mobility and strain energy in the film. The TiN film grows in closed packed (111) plane with the lowest strain energy. Since the dcMS and MPPMS TiN film possess high deposition rate, the growth of (111) plane is restricted and (220) plane with the lowest stopping energy becomes preferred orientation. Besides, as ionization rate and flux of plasma increase for MPPMS, high energy ion etching process will also restrict the growth of (111) and (200) plane, and (220) plane becomes preferred orientation.

Fig.3 shows surface and cross-sectional SEM micrographs of TiN films. The TiN film deposited by dcMS exhibits a large amount of columnar structures throughout the film thickness, and the surface clearly reveals pyramid-like micro particles with size of 300~500 nm. Voids and gaps between columnar structures are clearly observed. The surface roughness is 58 nm (Table 2). In comparison, the TiN film deposited by HPPMS and MPPMS shows dense and uniform columnar structures. The width of columnar structure decreases to 100~300 nm, which is considerably thinner than that of dcMS. The surface of TiN films deposited by HPPMS and MPPMS reveals rice-like and pyramid-like micro particles, and the surface roughnesses are measured to be 15 and 19 nm, respectively.

During magnetron sputtering process, current of gas discharge is produced by two mechanisms. They are ion attracted to target by negative potential from plasma nearby and secondary electron emitted from ion bombardment. The $n'(t)$ is assumed to be the total ion density in plasma at any time t , β is the percentage of ion attracted back to target ($0 < \beta < 1$), and γ is the average secondary electron emission coefficient of target. The discharge current $I(t)$ at time t is given by Eq.(1)^[25].

$$I(t) = \int n'(t) \beta (1 + \gamma) dA \quad (1)$$

where A is the target area. The evolution of ion density is determined by ion generation and annihilation. Ion generation is attributed to ionization of target and gas atom. Ion annihilation is conducted by two ways. They are the reverse attraction caused by negative target potential and ion

Table 2 Mechanical and corrosive properties of TiN films

| Technique | Ti/N ratio | Grain size/nm | Residual stress/GPa | Roughness/nm | Hardness, H/GPa | Young's modulus, E/GPa | H/E |
|-----------|------------|---------------|---------------------|--------------|-----------------|------------------------|-------|
| dcMS | 0.73 | 14 | 0.3 | 58 | 14 | 289 | 0.048 |
| HPPMS | 0.73 | 15 | -0.1 | 15 | 23 | 284 | 0.081 |
| MPPMS | 0.78 | 19 | -0.2 | 19 | 24 | 278 | 0.086 |

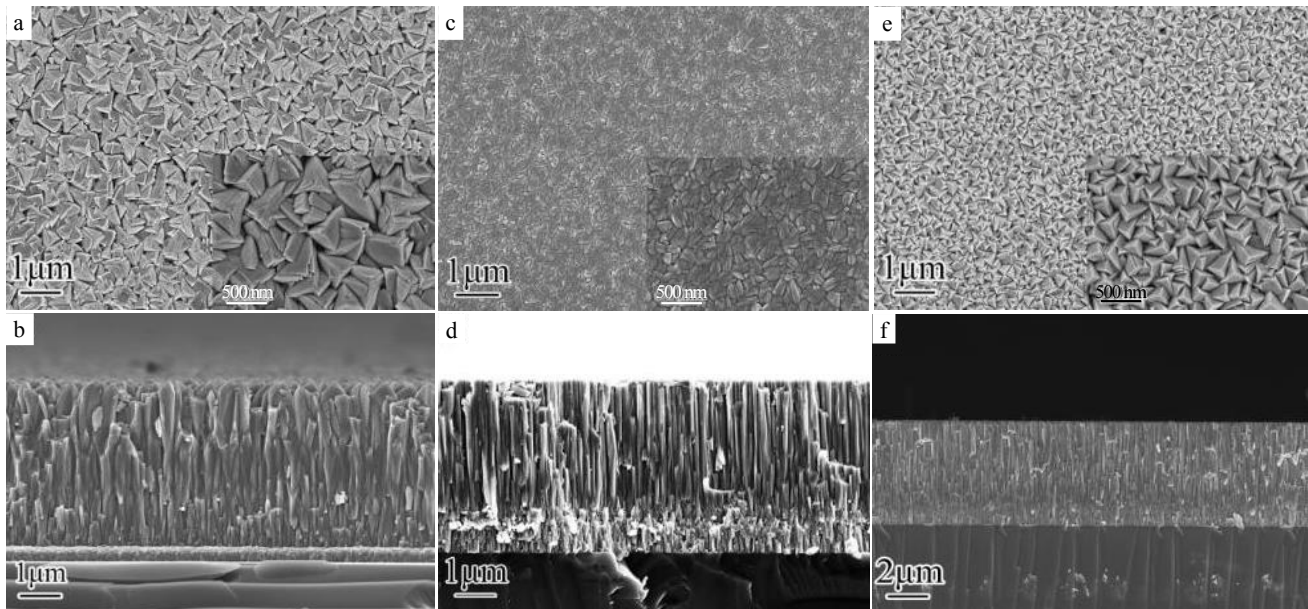


Fig.3 Surface and cross-sectional SEM micrographs of TiN films deposited by dcMS (a, b), HPPMS (c, d), and MPPMS (e, f)

recombination of ions and electrons in the plasma. Therefore, $I(t)$ is proportional to $n'(t)$.

In the deposition process of dcMS, the glow discharge produces smaller $I(t)$. The quantity of ions in the plasma is lower, and the sputtered Ti^+ ion is rare. The dcMS plasma with low ion flux is not able to provide sufficient ion bombardment and heat substrate. Based on the nucleation theory, low substrate temperature increases free energy difference of phase transition, thereby decreasing critical radius of nucleation and generating massive nucleation sites. As a result, the TiN film deposited by dcMS exhibits nanocrystalline structure and small grain size. Moreover, according to Thornton's microstructure classification^[26], the low substrate temperature and adatom mobility lead to porous microstructure containing large columnar structure in the film (Fig.3b).

HPPMS and MPPMS techniques aim to obtain high density plasma by applying pulsed high peak target power. Under the condition of high target power, many target atoms can leave target surface by sputtering and evaporation/sublimation, and be ionized by impact ionization in cathodic sheath. Therefore, the HPPMS and MPPMS deposition can obtain abundant deposited ions with high kinetic energy (5~20 eV)^[17]. High kinetic energy is transferred from deposited ions to adatom on substrate surface. It can improve adatom mobility and substrate temperature, which increases critical nucleation size of the film. Consequently, grain size of TiN films deposited by HPPMS and MPPMS is larger than by dcMS. Furthermore, adatoms with high mobility can diffuse into voids and gaps between columnar structure, so the TiN film is densified and smoothed. Enhanced ion bombardment restricts the coarsening of the columnar structure and makes the film surface smooth. Therefore, the TiN film deposited by HPPMS and MPPMS have dense columnar structure and smooth

surface.

2.3 Mechanical properties

Hardness (H) and Young's modulus (E) of TiN films are summarized in Table 2. H/E ratio is evaluated as an important and valuable parameter for the TiN film performance. High H/E value is expected to allow redistribution of applied load over a large area to delay failure^[27]. The TiN film deposited by dcMS shows the lowest hardness of 14 GPa and the highest Young's modulus of 289 GPa, resulting in a low H/E value of 0.048. The TiN films deposited by HPPMS and MPPMS show the similar hardness (23 and 24 GPa), Young's modulus (284 and 278 GPa), and H/E value (0.081 and 0.086).

For the same film, the hardness is mainly influenced by the microstructure, such as grain size^[28], compressive stress, phase segregation^[29], element substitution^[30], compactness^[31] and amorphous phase^[32]. All TiN films have a similar Ti:N ratio in a range of 0.73~0.78. Therefore, compressive stress and compactness become the main factors. Higher hardness and H/E value are attributed to the higher compressive stress and structure densification caused by stronger ion bombardment and higher ion kinetic energy from highly ionized plasma in HPPMS and MPPMS deposition process.

Adhesion of TiN films was evaluated via critical load (L_c) in microscratch test. L_c is an instant applied load when the film firstly cracks, chips or delaminates^[33]. Scratch track images are presented in Fig.4, which shows obvious failure events. L_c values of TiN films deposited by dcMS, HPPMS and MPPMS are 6, 10 and 12 N, respectively. First crack of the film deposited by dcMS occurs at the edge of scratch track with low L_c , due to different toughness between the TiN film and substrate. Massive lateral cracks along the side of scratch track are observed in Fig.4a, as applied load increases. As shown in Fig.4b, the TiN film deposited by HPPMS exhibits a

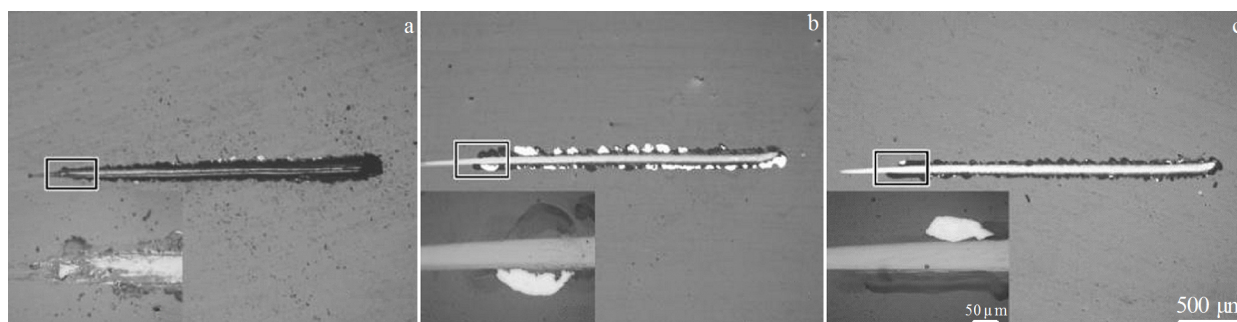


Fig.4 Scratch track morphologies of TiN films deposited by dcMS (a), HPPMS (b), and MPPMS (c)

higher L_c , and the film shows a few delaminations and chips at the edge of scratch track. A slightly improved adhesion is shown in the film deposited by MPPMS, and the delaminations exist at the edge of scratch track, as shown in Fig.4c.

Adhesion is mainly influenced by the residual stress, ion density and film thickness^[34-36]. In general, adhesion is enhanced by decreasing the residual tensile stress or increasing the residual compressive stress slightly. High density plasma can enhance adhesion, because it can not only produce dense film, but also increase ion bombardment onto substrate surface. And increasing film thickness can improve adhesion. Due to a low density plasma and the residual tensile stress of 0.3 GPa, the TiN film deposited by dcMS shows a poor adhesion. The main reason for the improvement of the adhesion of TiN films prepared by MPPMS is the compact microstructure, compressive stress and high density plasma.

3 Conclusions

1) TiN film deposited by direct current magnetron sputtering (dcMS) exhibits a porous columnar structure, which give rises to poor mechanical properties. High power pulsed magnetron sputtering (HPPMS) and modulated pulsed power magnetron sputtering (MPPMS) techniques can improve ion flux and ion energy of plasma under the condition of high peak target power.

2) The TiN films deposited by HPPMS and MPPMS exhibit smooth surface, dense columnar structure and fine grain size. The films have high hardness (23 and 24 GPa) and H/E ratio (0.081 and 0.086). But the average deposition rate of TiN films deposited by MPPMS is close to that of dcMS and significantly higher than that of HPPMS.

References

- Chawla V, Jayaganthan R, Chawla A K et al. *Journal of Materials Processing Technology*[J], 2009, 209(7): 3444
- Lin N M, Huang X B, Zhang X Y et al. *Applied Surface Science* [J], 2012, 258: 7047
- Lin J L, John J, Moore J J et al. *Surface & Coatings Technology* [J], 2010, 204(14): 2230
- Lin J, Moore J J, Sproul W D et al. *Journal of Vacuum Science & Technology A*[J], 2011, 29: 61 301
- Greczynski G, Mraz S, Hultman L et al. *Applied Physics Letters* [J], 2016, 108: 41 603
- Kouznetsov V, Macák K, Schneider J M et al. *Surface & Coatings Technology*[J], 1999, 122(2-3): 290
- Bagcivan N, Bobzin K, Grundmeier G et al. *Thin Solid Films*[J], 2013, 549: 192
- Wu Z Z, Tian X B, Gong C Z et al. *Surface & Coatings Technology*[J], 2013, 229: 210
- Brenning N, Huo C, Lundin D et al. *Plasma Sources Science & Technology*[J], 2012, 21(2): 25 005
- Anders A. *Journal of Vacuum Science & Technology A*[J], 2010, 28: 783
- Sidelev D V, Bleykher G A, Grudin V A et al. *Surface & Coatings Technology*[J], 2018, 334: 61
- Bleykher G A, Borduleva A O, Krivobokov V P et al. *Vacuum*[J], 2016,132: 62
- Yang C, Jiang B L, Feng L. *Acta Metallurgica Sinica*[J], 2015, 51: 1523
- Ma C H, Huang J H, Chen H. *Thin Solid Films*[J], 2004, 446: 184
- Zenoozi S, Agbolaghi S, Poormahdi E et al. *Macromolecular Research*[J], 2017, 25: 826
- Li G D, Li L H, Han M Y et al. *Metals*[J], 2019, 9: 918
- Shekargoftar M, Jurmanova J, Homola T. *Metals*[J], 2019, 9: 991
- Alexis D M, Schuster F, Billard A et al. *Surface & Coatings Technology*[J], 2017, 330: 241
- Greczynski G, Hultman L. *Vacuum*[J], 2016,124: 1
- Zhang L N, Chen L Y et al. *Metals*[J], 2019, 8: 850
- Supplit R, Koch T, Schubert U. *Corrosion Science*[J], 2007, 49: 3015
- Du H, Zhao H, Xiong J. *International Journal of Refractory Metals & Hard Materials*[J], 2013, 37: 60
- Lin J L, Moore J J, Sproul W D et al. *Surface & Coatings Technology*[J], 2020, 203: 2230
- Lang F Q, Yu Z M. *Surface & Coatings Technology*[J], 2001, 145: 80
- Lin J L, Sproul W D, Moore J J. *Surface & Coatings Technology*

- [J], 2012, 206: 2474
- 26 Pharr G M, Oliver W C. *Mrs Bulletin*[J], 1992, 17: 28
- 27 Anders A. *Surface & Coatings Technology*[J], 2010, 204: 2864
- 28 Ni W, Cheng Y T, Lukitsch M J et al. *Applied Physics Letters*[J], 2004, 85: 4028
- 29 Zhao Y H, Guo C Q, Yang W J et al. *Vacuum*[J], 2015, 112: 46
- 30 Sergueeva A V, Stolyarov V V, Valiev R Z et al. *Scripta Mater* [J], 2001, 45: 747
- 31 Stallard J, Poulat S, Teer D G. *Tribology International*[J], 2006, 39: 159
- 32 Wu Z Z, Xiao S, Ma Z Y et al. *AIP Advances*[J], 2015, 5: 97 178
- 33 Mukherjee S, Gall D. *Thin Solid Films*[J], 2013, 527: 158
- 34 Lin J L, Moore J J, Mishra B et al. *Surface & Coatings Technology*[J], 2008, 202: 1418
- 35 Laing K, Hampshire J, Teer D et al. *Surface & Coatings Technology*[J], 1999, 112 : 177
- 36 Heinke W, Leylan A, Matthews A et al. *Thin Solid films*[J], 1995, 270: 431

不同磁控溅射工艺对纳米晶 TiN 薄膜微观结构与力学性能的影响

郝娟¹, 杨超¹, 蒋百灵¹, 杜玉洲¹, 王戎¹, 王旭¹, 周克崧²

(1. 西安理工大学材料科学与工程学院, 陕西 西安 710048)

(2. 广东省科学院新材料研究所, 广东 广州 510651)

摘要: 对比研究了直流磁控溅射 (dcMS)、高功率脉冲磁控溅射 (HPPMS) 和调制脉冲磁控溅射 (MPPMS) 所沉积纳米晶 TiN 薄膜的组织结构与力学性能。结果表明, 因 dcMS 溅射粒子离化率与动能均较低, 薄膜表现为存在少量空洞的柱状晶结构, 薄膜力学性能差、沉积速率为 51 nm/min。HPPMS 因具有较高的瞬时离化率和较低的占空比, 薄膜结构致密而光滑, 性能得到了显著改善, 但平均沉积速率较低, 仅为 25 nm/min。通过 MPPMS 技术可大范围调节峰值靶功率和占空比, 从而得到较高的离化率和平均沉积速率, 薄膜结构致密光滑、力学性能优异, 沉积速率达 45 nm/min, 接近 dcMS。

关键词: MPPMS; TiN 薄膜; 显微组织; 沉积速率

作者简介: 郝娟, 女, 1990年生, 博士, 西安理工大学材料科学与工程学院, 陕西 西安 710048, 电话: 029-82312315, E-mail: haojuan19901207@163.com